Numerical Modelling and Structural Analysis of Armoury Museum at City Palace Udaipur, Rajasthan, India

Omkar S. Adhikari[1](✉) and João M. Pereira[2]

[1] Indian National Trust for Art and Cultural Heritage, Lodi Road, New Delhi, India
adhikariomkar@gmail.com
[2] ISISE – Institute for Sustainability and Innovation in Structural Engineering), University of Minho, Campus de Azurem, Guimarães, Portugal
jpereira@civil.uminho.pt

Abstract. The work intends to study and analyse a case study of the City Palace Udaipur in Rajasthan, India. The City Palace complex, Udaipur is an exemplary model of the Rajput palace fortress and its construction lasted 400 years, starting from 1553C.E [1]. The Saleh Khana (armoury museum) had been intervened due to the presence of structural damage [2]. This work focusses on the analysis of the structural condition of the Saleh Khana (armoury museum), within the City Palace of Udaipur, India. In general, two main objectives are achieved. First, the modelling and assessment of the condition of the structure before the interventions are carried out. The obtained results are then compared with the documented damage present in the structure before the interventions to verify if the damage present at the structure was reflected properly while modelling and its only due to the vertical forces acting on the building. Secondly, the modelling and assessment of the condition of the structure after the interventions is carried out. The obtained results are then compared with structural analysis before the intervention to verify the improvements made with the interventions that were proposed and executed. To achieve these objectives, different 3D finite element models of the structure were analysed. The research was able to justify several important damage features of the building. Particularly, good consistency was obtained regarding the damage patterns of the stone frames and the vaulted roofs. Furthermore, the results indicate that the numerical model developed within the scope of this work can properly replicate the overall behaviour of the structure. The efficiency of the interventions executed in the Saleh Khana was estimated, and an improvement on the overall capacity of the structure under vertical loads of 67% can be expected.

Keywords: FE modelling · Structural Analysis · Masonry structures · Stone masonry · Non-linear static analysis

1 Salehkhana – Armory Museum

The city palace complex is a monumental site with an ensemble of built form and courtyard spaces at varying levels built on a over the time period of 400 years. Salehkhana was built in 16th century CE, comprises of a series of vaulted spaces with smaller vaulted

Y. Endo and T. Hanazato (Eds.): SAHC 2023, RILEM Bookseries 46, pp. 387–399, 2024.
https://doi.org/10.1007/978-3-031-39450-8_32

rooms (a Fig. 1) which served as the waiting hall for the guests that came to meet the King [2].

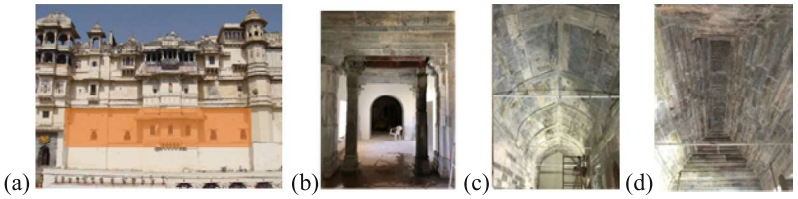

Fig. 1. Salehkhana: (a) main façade highlighting Salehkhana area; (b) interior openings; (c) main vault; (d) corbelled stone vaults.

In current scenario Salehkhana is partially functioning as an Armoury gallery in Mardana Mahal, City Palace Museum. The revised museum plan focused on the restoration of the Salehkhana to its original Grandeur by removing additions and alteration done due to structural distress in later periods in past. The proposal intended to improve the structural safety of the existing structure, also regain the long-spanned hall spaces while reorganizing circulation pattern. to crater museum theme.

1.1 Defect Mapping

Detail measured drawings and photographic survey were primary mode of data collection and defect identification. The observations were reflected on drawing in form of defect maps. Damage observed were of two types: a) opening of joints between adjacent stones (Fig. 2a); b) structural cracks (Fig. 2b). The alarming damage observed (Fig. 2) were the cracks in the stone beams (within stone frames).

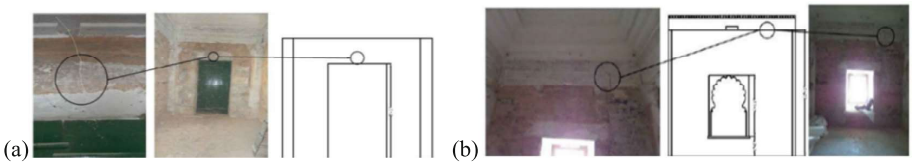

Fig. 2. Defect examples: (a) cracks: center of top beam (b) opening of joints: side walls

1.2 Proposed Interventions

Based on detail assessment, It was difficult to revert back to original opening size by removing total infill due to heavy loading and existing crack in stone beam above Therefore, mid-way was suggested to introduce additional system which support the crack beam and help to increase opening size for museum. The two systems were introduced firstly Arch system with width of opening is 1.2 m (3 stone beams) and second system of steel frame with 0.8 m (2 stone beams).

During scientific investigation historic decorative stone column were found embedded in the infill wall. Thus, the proposal was revised from stone arches in all four frames to only two stone arches (marked in red) and two steel frames (marked in yellow) making the columns visible for the visitors (Fig. 3).

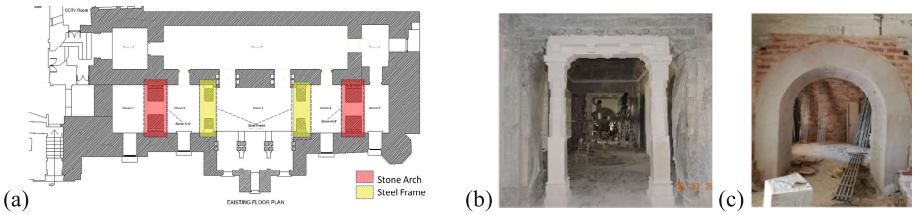

Fig. 3. (a) Location of the interventions. (b) steel frame system (c) Arch system

1.3 Numerical Modelling

In this case Finite Element Modelling was performed using DIANA10.2 software. Due to simplicity and the lesser calculation requirements, macro modelling approach was used for the analysis of the Salehkhana structure. The model was constructed using 3D solid elements. Building the geometry of the model is an important and complex task as there is, often, no distinction between decorative and structural elements. Due the complexity of historic construction and several simplifications in geometry were assumed. Here, the focus was to keep the geometry idealization as simple as possible, while being able to properly reproduce the behavior of the structure. Some of the simplification undertaken while building the model can be seen in (Fig. 4).

Fig. 4. (a) simplification of the corbelled roof; (b) stone columns.

Besides this kind of geometrical simplifications, one important simplification was the fact that only the ground floor was modelled. Because only vertical loads are to be considered in this analysis, only the first floor was modelled. However, the weight from the upper floors was considered by introducing additional elements aligned with the walls from the upper floors. These extra elements were considered linear elastic but with specific densities that take into account the extra weight of the upper floors.

1.4 Modelling Procedure

The modelling procedure was as follows (Fig. 5): a) A simplified floor plan was firstly drawn in CAD and latter imported to DIANA; b)The stone columns and beams were added; c)The floor plan was extruded in height forming the walls of the structure; d)With the walls created, the openings were introduced; e)The vaults were created and attached to the structure; f)The remaining of the roof structure (filling) was built; Additional blocks were created aligned with the walls from the upper floors in order to apply the load from the upper floors.

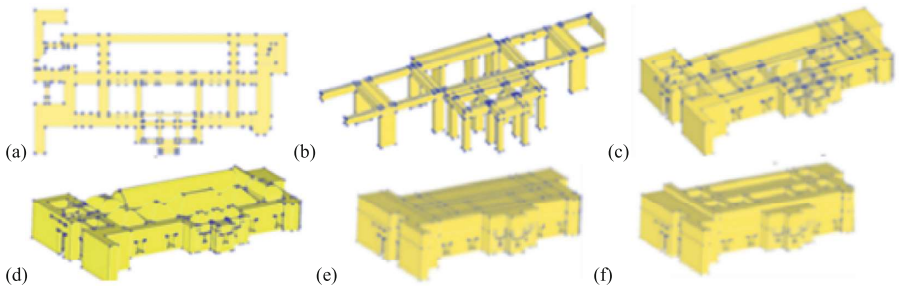

Fig. 5. The modelling procedure

1.5 Loads and Boundary Conditions

Regarding the loads, two different types of loads were considered: a) self-weight; b) hydrostatic pressure. The procedure of applying the loads was first, the self-weight of the structure was applied to the model (100%), then hydrostatic pressure was applied to the retaining walls (100%), then self-weight of the structure was increased gradually until the structure presented excessive damage (>100%). The hydrostatic pressure was considered since the building is inserted in a mountain, having certain walls in direct contact with the soil (retaining walls) (Fig. 6).

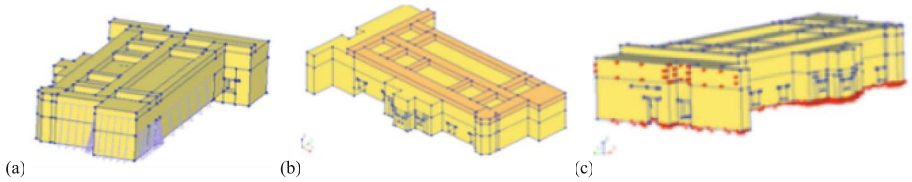

Fig. 6. (a) Numerical model with the hydrostatic pressure on the retaining walls, (b) Numerical model with the extra elements with equivalent densities for the extra mass, (c) Numerical model with the support conditions.

Because the 3D model only considered the first floor of the structure and the weight from the upper floors, as well as the roof needed to be taken into consideration in the analysis, the second, the total mass of the upper floors (walls and roofs) and top domes was estimated considering their volume and their specific mass and was added above each wall and with help of mass unloading on each wall, it was possible to calculate an equivalent density for the extra elements considering the total mass of the upper floors. This was only possible because only vertical loading was considered in the analysis. Because the building lays on top of a very thick stone layer (>2 m), the model was considered pinned at the bottom of its walls and columns. Additional supports were placed on the south end of the structure and the displacement in the XX direction was blocked, considering the connection of the building to the remaining adjacent structures.

1.6 Meshing

Four different types of regular solid elements were employed for meshing the numerical model: a) eight-node isoparametric solid brick element; b) five-node isoparametric solid pyramid element; c) four-node, The HX24L an eight-node isoparametric solid brick element; d) six-node isoparametric solid wedge element. The final mesh was composed of 369662 nodes and 65652 elements. The distribution of element types can be seen in (Fig. 7).

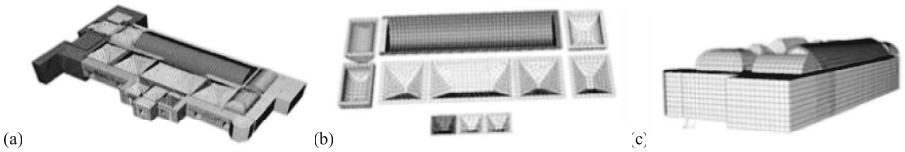

Fig. 7. Mesh in DIANA: (a) Bottom view (b) roof; (c) corner

1.7 Constitutive Material Laws and Mechanical Properties

The non-linear behavior of masonry was modeled using a total strain based constitutive model – Total Strain Crack model [3]. The input for the Total Strain Crack model, in its rotating form, comprises two parts: (1) the definition of the behavior in tension and compression, and the corresponding non-linear material properties; and (2) the basic parameters and linear-elastic properties such as material density, Young's modulus and Poisson's ratio. The fracture energy is defined as the energy necessary to create a unit area of a fully developed crack (Fig. 8).

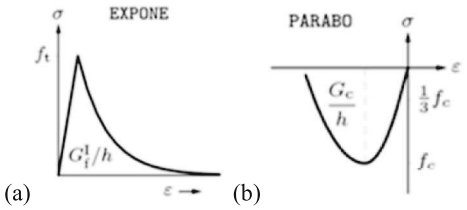

Fig. 8. Stress-strain curves: (a) Exponential softening curve for tensile masonry behavior; (b) parabolic curve for compressive masonry behavior.

Due to the lack of information regarding the physical and mechanical properties of masonry present at Salehkhana, typical values were estimated and adopted based on the literature [4]. Only for the compressive strength of the granite stones (monolithic stone) tests were performed and a value of 21.16 MPa was available. In this model there are three types of materials to be considered and the final mechanical properties assumed in the model can be seen in Table 1: a) Ashlar masonry with good bond and lime mortar joint. It is a three-leaf wall made with rectangular stone unit. It is located on the west end of the Salehkhana (Fig. 9a); b) Rubble masonry with small irregular units and a good quality thick mortar joint. The wall is three-leaf with thickness of 1.2 to 1.6 m (Fig. 9b); c) Monolithic stone (granite).

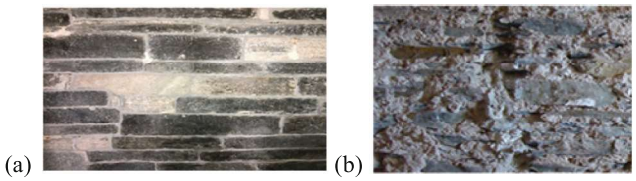

Fig. 9. Types of masonry considered in model: a) ashlar masonry; b) rubble masonry.

The values for the density, compressive strength and Young's Modulus were taken directly from the available literature. The tensile strength was assumed as 7% to 10% of the compressive strength. As far as the softening behavior of masonry is considered, the tensile and compressive fracture energy values, necessary for the presented constitutive models, can be derived according to the tensile and compressive strength and each ductility index, according to:

$$d = G/f \tag{1}$$

For the compressive fracture energy [5], it is suggested a value of d = 1.6 mm for compressive strength lower than 12 MPa. The recommendation [6] is to increase this value for lower strength materials (typically more ductile):

$$d = 2.8 - 0.1 f_c[mm] \tag{2}$$

For the tensile fracture energy, no relation can be found between strength and fracture energy and a value of 0.02 N/mm is recommended [7].

Table 1. Mechanical properties assumed in the numerical model.

Mechanical property	Ashlar masonry	Rubble masonry	Granite stone
E (Young's modulus) [MPa]	2400	1020	12243
f_c (Compressive strength) [MPa]	4.00	1.50	21.16
G_c (Fracture energy) [N/mm]	9.60	3.98	24.0
f_t (Tensile strength) [MPa]	0.30	0.10	1.97
G_f (Fracture energy Mode-I) [N/mm]	0.02	0.01	0.02
ρ (density) [kg/m^3]	2200	2000	2700

1.8 Results for Non-linear Analysis Before Intervention

In order to track the behavior of the structure during the analysis, several nodes were highlighted and tracked (Fig. 10). These are nodes in the stone beams (center and ends) and center of the vaults. These nodes were chosen considering the defect map previously presented and in which most of the damage was concentrated in the stone frames and roofs (vaults) (Fig. 11).

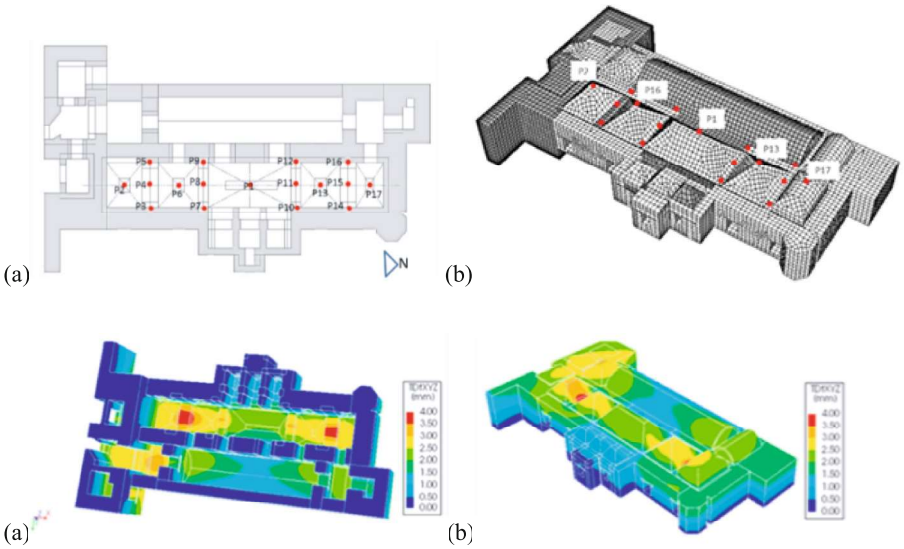

Fig. 10. Interest nodes: (a) plan view schematic; (b) 3D view, Deformed mesh at maximum displacement: a) 3D top view; b) 3D bottom view.

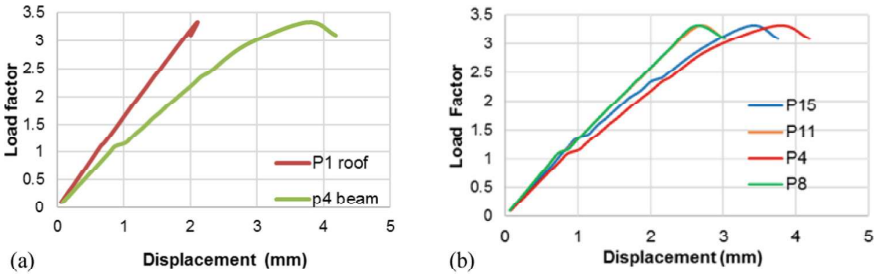

Fig. 11. (a) Comparison of displacement curves between center of stone beam (P4) and center of vault (P1), (b) Comparison of displacement curves between all stone beams.

In order to identify the location of the damage within the structure, the maximum principal strains were used. From the numerical model it was possible to see that the stone frames and the vaults were the areas with the highest maximum principal strains. Figure 12 shows the maximum principal strains at maximum displacement for the stone frames was shown in the model (Fig. 13a) and it is possible to see that in the stone frames, the damage is concentrated at the center point of the beam. In the vaults (Fig. 13b), the damage is concentrated on the top edge of the vault, and some cracks are starting from the corners moving towards the center. In the rest of the structure, it was possible to see that the masonry walls did not show any considerable damage (Fig. 13c).

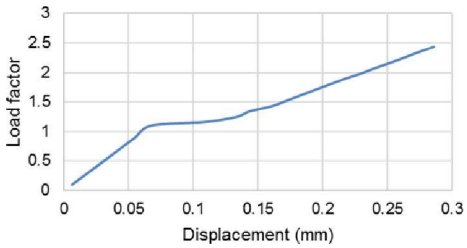

Fig. 12. Opening of stone frame with node P8.

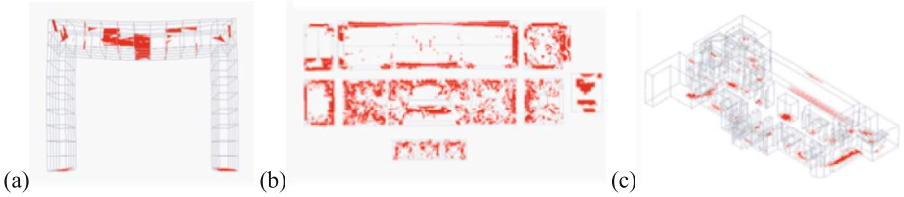

Fig. 13. Maximum principal strains: a) stone frame with node P4; b) vaults (bottom view); c) masonry walls (same color scale).

1.9 Numerical Model vs. Defect Map

One of the objectives was comparing the results of the non-linear static analysis using finite element method with the damaged identified within the real structure. So, if damage patterns were similar, it would be possible to assume that the damage present in the structure is only due to the vertical loads acting on the structure. From the defect mapping it was seen that the areas with the most damage were the stone frames and the vaults. And this was concluded in the numerical model as well (Fig. 14).

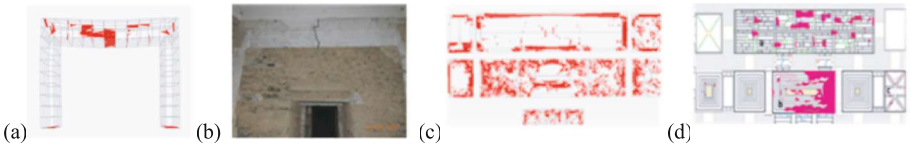

Fig. 14. Comparison of damage for the stone frames: (a) FEM with maximum principal strains; (b) crack at center point of stone beam. Comparison of damage for the vaults: (c) FEM with maximum principal strains; (d) crack distribution.

Some areas in the numerical model seem more damaged when compared with the damage map of the existing structure. However, this can be explained by the existence of a decorative cover of plaster within the vaults, making it possible that not all damage is visible.

1.10 Non-linear Structural Analysis After Intervention

The second analysis was the structural analysis of the structure after the interventions. Here, the objective is to quantify the influence of the interventions in the overall capacity of the structure considering vertical loading.

The second analysis was the structural analysis of the structure after the interventions. Here, the objective is to quantify the influence of the interventions in the overall capacity of the structure considering vertical loading.

1.11 Numerical Modelling

The addition of two different substructures was done in existing model: a) two stone arches; b) two steel frames. (Fig. 15) shows the introduction of the substructures into the base model and Fig. 16 show finite element mesh used for these sub-structures. For the stone arch, the material properties of the existing rectangular stone masonry were used (Table 1), for the steel a linear elastic behavior was used with a Young's Modulus of 200 GPa.

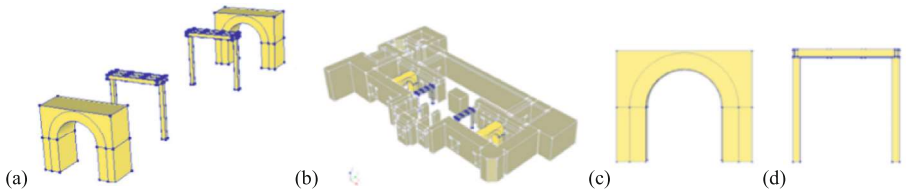

Fig. 15. (a) building the sub-structures considered in the intervention; (b) placing the sub-structures into the base model; (c) front view of the stone arch geometry; (d) front view of the steel frame geometry.

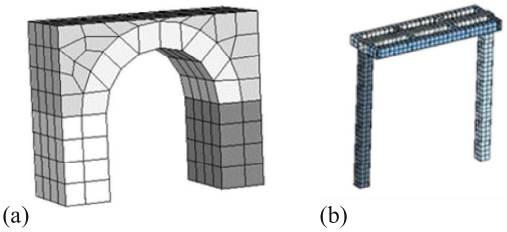

Fig. 16. Finite element mesh of the sub-structures: a) stone arch; b) steel frame.

1.12 Results for Non-linear Analysis After Intervention

To assess the structural behavior of the building, a static non-linear analysis is performed for vertical loading, using the finite element software DIANA 10.2. The procedure for applying the load was the same as the one presented in the previous Section. The overall capacity of the structure to vertical loads is 5.56 g (Fig. 17), meaning that is 5.56 times its own self-weight. The deformed mesh of the building at maximum displacement can be seen in (Fig. 18).

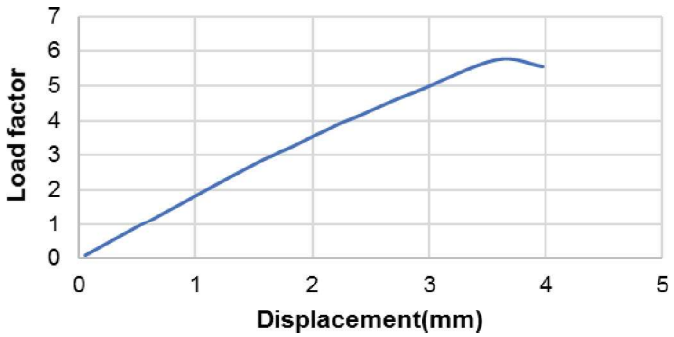

Fig. 17. Vertical load factor vs. displacement at node P8 (beam).

It is possible to see that the behavior of the structure differs from the structure before interventions. The frames with the highest displacement are now the frames with the steel reinforcement frame and the stone arches (Fig. 19).

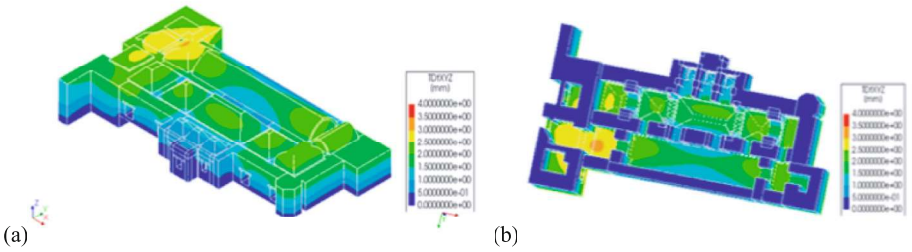

Fig. 18. Deformed mesh at max displacement: (a) 3D top view; (b) 3D bottom view.

Similarly, to the previous model, in order to identify the location of the damage within the structure, the maximum principal strains were used. From the numerical model, it was notice that the intervention is having the desired effect, lowering the strain values at the center of the beams (Fig. 20a). The strain in the roof reduced and it does not show any further damage pattern (Fig. 20b). The masonry walls also did not have any considerable strains as before (Fig. 20c).

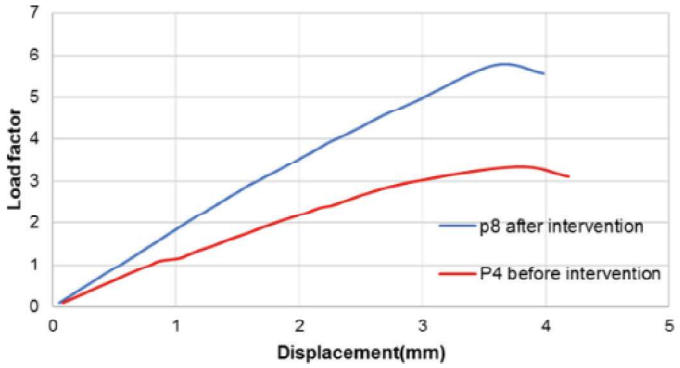

Fig. 19. Comparison of displacement curves between center of stone beam (P4) and (P8).

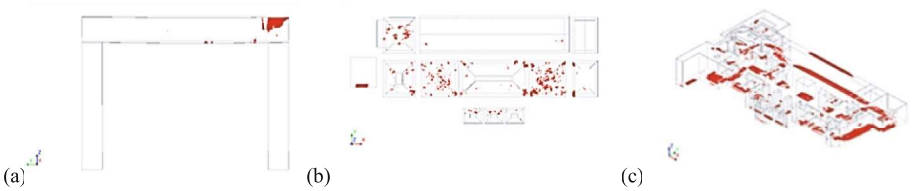

Fig. 20. Maximum principal strain: (a) stone frame at node P8; (b) vaults (bottom view); (c) masonry walls (same color scale).

1.13 Effectiveness of the Intervention Measures

In order to access the effectiveness of the intervention measures, both models were compared: a) before interventions; b) after interventions. Here, the comparison was performed in terms of capacity curves. (Fig. 21) shows the comparison in capacity curves for both models before and after the intervention at different locations of the structure. It was seen the model with the interventions presents an overall capacity 1.67 times greater than the overall capacity of the model before the interventions. In fact, this can be translated as a 67% improvement in the overall capacity of the structure.

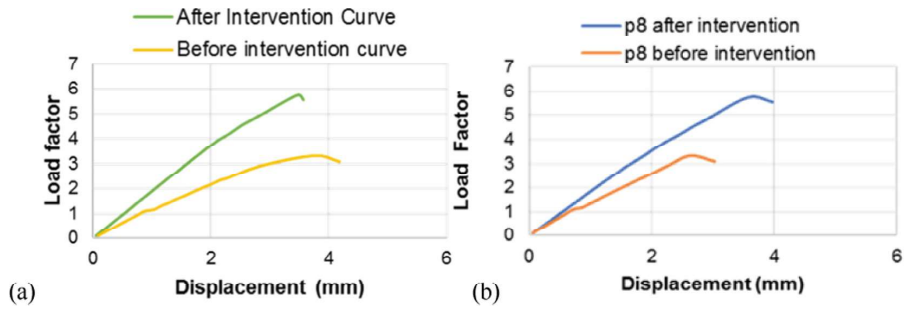

Fig. 21. Comparison of capacity curves for models before and after the interventions: (a) Node P8; (b) node P8.

2 Conclusions

In general, two main objectives were achieved. The first objective was modelling and assessment of the Salehkhana before the interventions. The results of this non-linear static analysis were compared with the damage map of the structure.

The second objective was modelling and assessment of the Salehkhana after the interventions. The results of this assessment were compared with the results of the analysis before the interventions so that the effectiveness of the proposed intervention could be assessed. Based on the works, the following conclusions can be formulated:

a) The 3D non-linear numerical model developed within the scope of this work is able to reproduce the overall behaviour of the Salehkhana structure.
b) By comparing the damage patterns of the numerical model and the defect map available from the structure before the intervention it was possible to conclude that the damage present at the structure is due to its own vertical loading.
c) From the result of 3D non-linear numerical model with the interventions it was possible to conclude that the performed interventions were able to increase the overall capacity of the structure by 67%.

Acknowledgement. I am thankful to all the Professors who taught me during the course, specially, to Professor Paulo B. Lourenço for guiding me during the course and sustained my choice of the

topic of the thesis. I am also grateful to Shriji Arvind Singh Mewar of Udaipur, Chairman and Managing Trustee, Maharana of Mewar Charitable Foundation (MMCF), The City Palace, Udaipur for his support and guidance during my stay in Udaipur. I am thankful to MMCF for scholarship and Dr. Shikha Jain for all the learning and experience they provided me in field of Conservation. Also thank you to Dr. Vaishali Latkar for always being my mentor and guide since my journey of conservation.

References

1. DRONAH: Conservation Master Plan an Overview. The City Palace Complex, Udaipur, Final Report, Maharana of Mewar Charitable Foundation, Udaipur, India, p. 84, Udaipur, India (2009)
2. MMCF: Detailed project Report Salehkhana Ground Floor and Salehkhana First Floor (Nikka-ki-Chopad): Arms and Armoury Related Exhibition. The City Palace Museum Udaipur, Rajasthan, India, Maharana of Mewar Charitable Foundation, 171 p. Udaipur, India (2015)
3. TNO DIANA (2009) DIANA, Displacement methods Analyser, release 9.4, User's Manual
4. NTC Norme tecniche per le costruzioni - Il Capo del Dipartimento della Protezione Civile. With Circolare no. 617 (2009). Il Ministro Delle Infrastrutture, Italy (in Italian) (2008)
5. MC 2010: fib Model Code 2010, first complete draft, vol-2. Fib bulletin 56, 17p. (2010)
6. Lourenço, P.B.: Recent advances in masonry modelling: micro modelling and homogenization. Multiscale Modeling in Solid Mechanics, pp. 251–294 (2009a)
7. Lourenço, P.B.: Recent advances in masonry modelling: micro modelling and homogenization. Multiscale Modeling in Solid Mechanics, pp. 251–294 (2009b)